Electronic Supplementary Information for

Chemically synthesized (Ag, Mn_2O_3)-codecorated ZnO nanparticles for achieving superior visible light-induced photodegradation and enhanced gas sensitive activity

Jing Li [a], Qiuping Zhang [a], Huan Yuan [a], Kaiyi Luo [a], Yutong Liu [a], Wenyu Hu [a], Ming Xu [a*], Shuyan Xu [b]

a College of Electrical &Information Engineering & Key Lab of Information Materials of Sichuan Province, Southwest University for Nationalities, Chengdu 610041, China. hsuming_2001@aliyun.com (M. Xu)

b Plasma Sources and Application Center/Space Propulsion Centre Singapore, NIE, and Institute of Advanced Studies, Nanyang Technological University, 637616, Singapore.

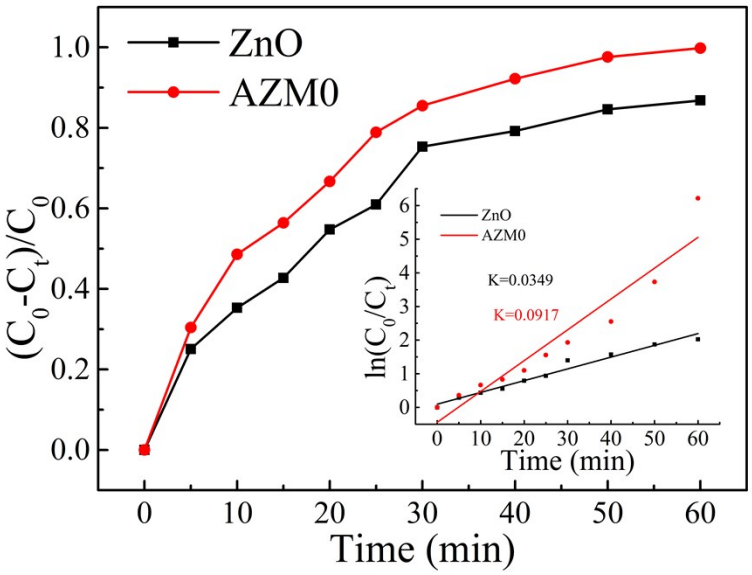

Fig. S1 Photodegradation curves and the corresponding first-order constants ($K= \ln(C_0/ C_t)$) of ZnO and AZM0 samples for the elimination of MB under simulated sunlight irradiation.

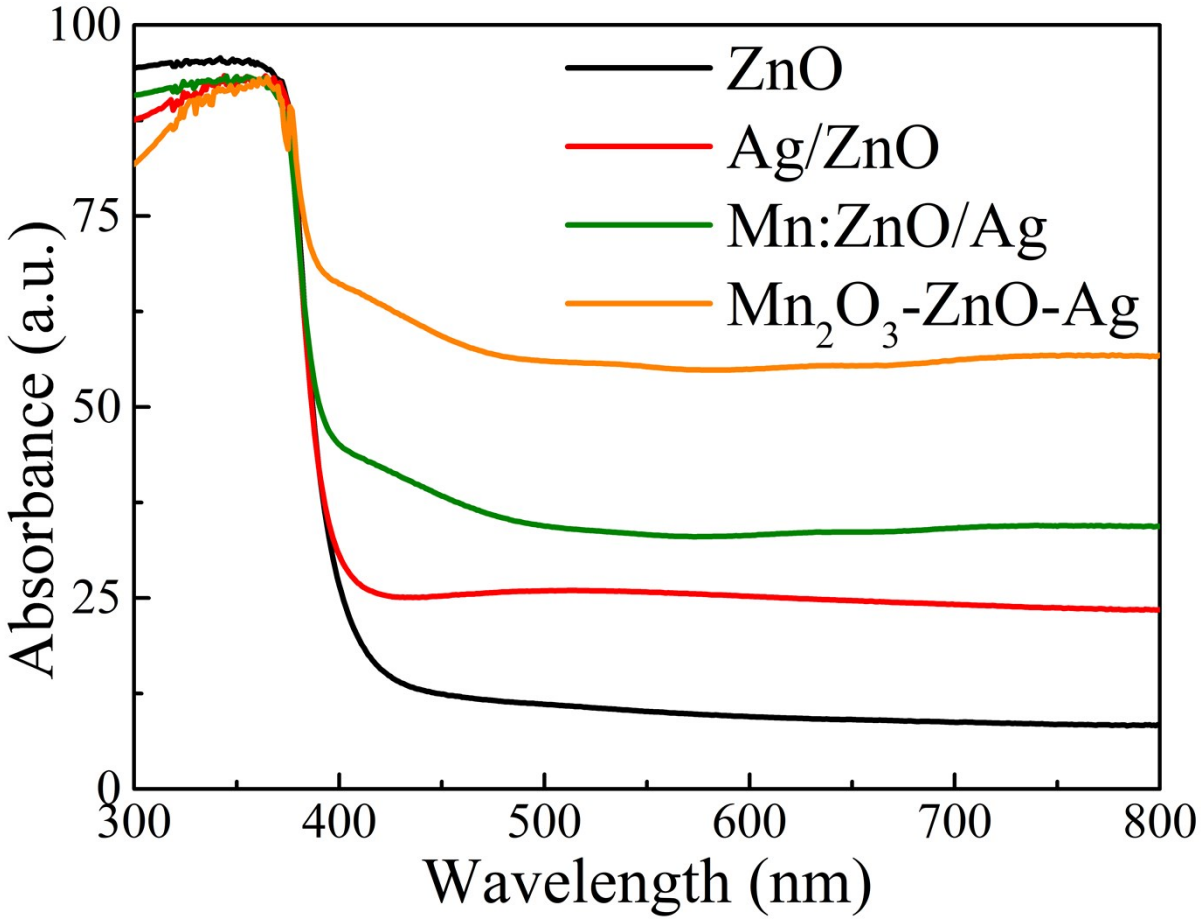

Fig. S2 UV-vis absorption spectra of pure ZnO, Ag/ZnO, Mn:ZnO/Ag and Mn_2O_3-ZnO-Ag samples.

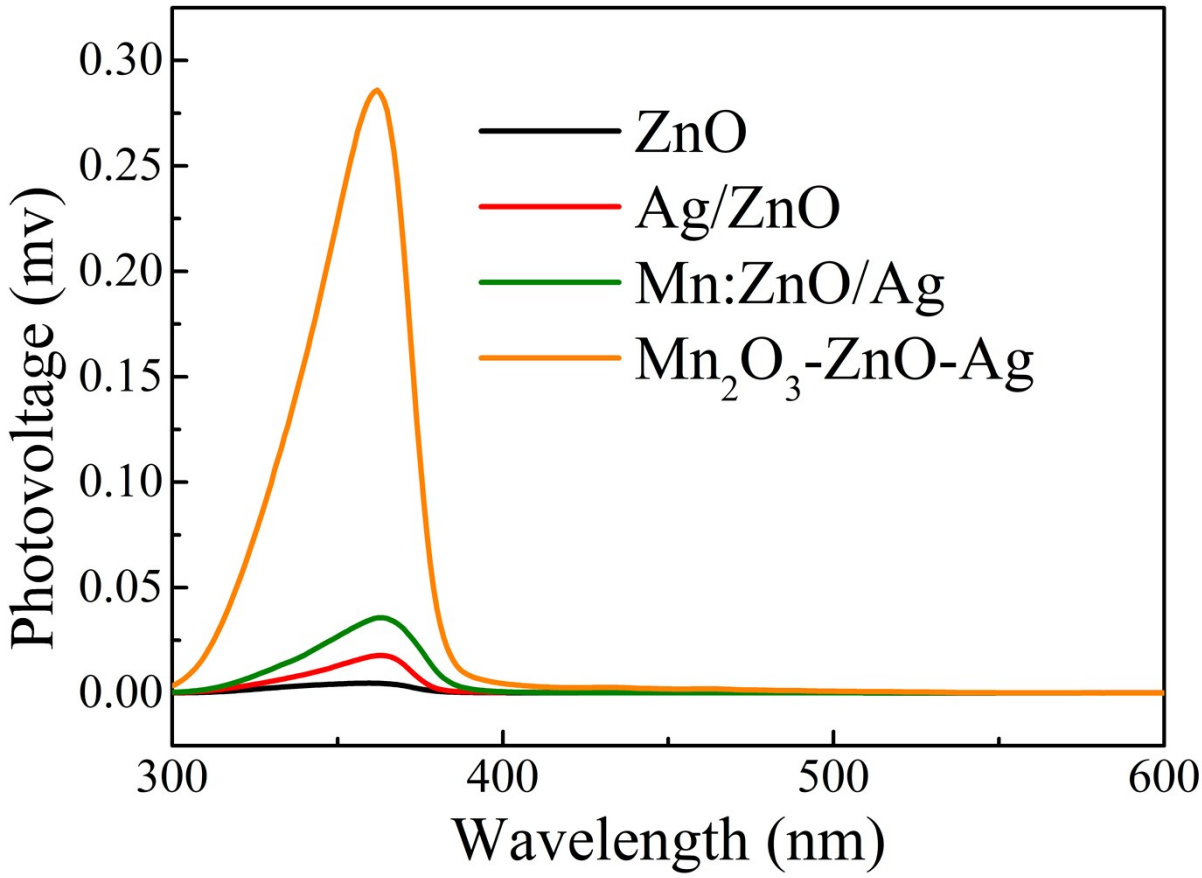

Fig. S3 SPV spectra of pure ZnO, Ag/ZnO, Mn:ZnO/Ag and Mn_2O_3-ZnO-Ag samples.

Table S1. The microstructural parameters and crystallite size of as-synthesized samples (θ, d, a, c, and D represent the diffraction angle, interplanar spacing, lattice parameters a and c, and the diameters of ZnO, respectively).

Samples	2θ(100)/°	d(100)/nm	d(002)/nm	d(101)/nm	a/nm	c/nm	D/nm
AZM0	31.78	0.2805	0.2600	0.2473	0.3253	0.5449	31.76
AZM1	31.78	0.2808	0.2601	0.2474	0.3255	0.5452	32.61
AZM3	31.76	0.2813	0.2605	0.2479	0.3258	0.5456	33.53
AZM5	31.76	0.2806	0.2603	0.2476	0.3254	0.5453	31.76
AZM7	31.78	0.2803	0.2598	0.2472	0.3251	0.5449	30.53
AZM10	31.76	0.2798	0.2590	0.2465	0.3245	0.5445	28.11

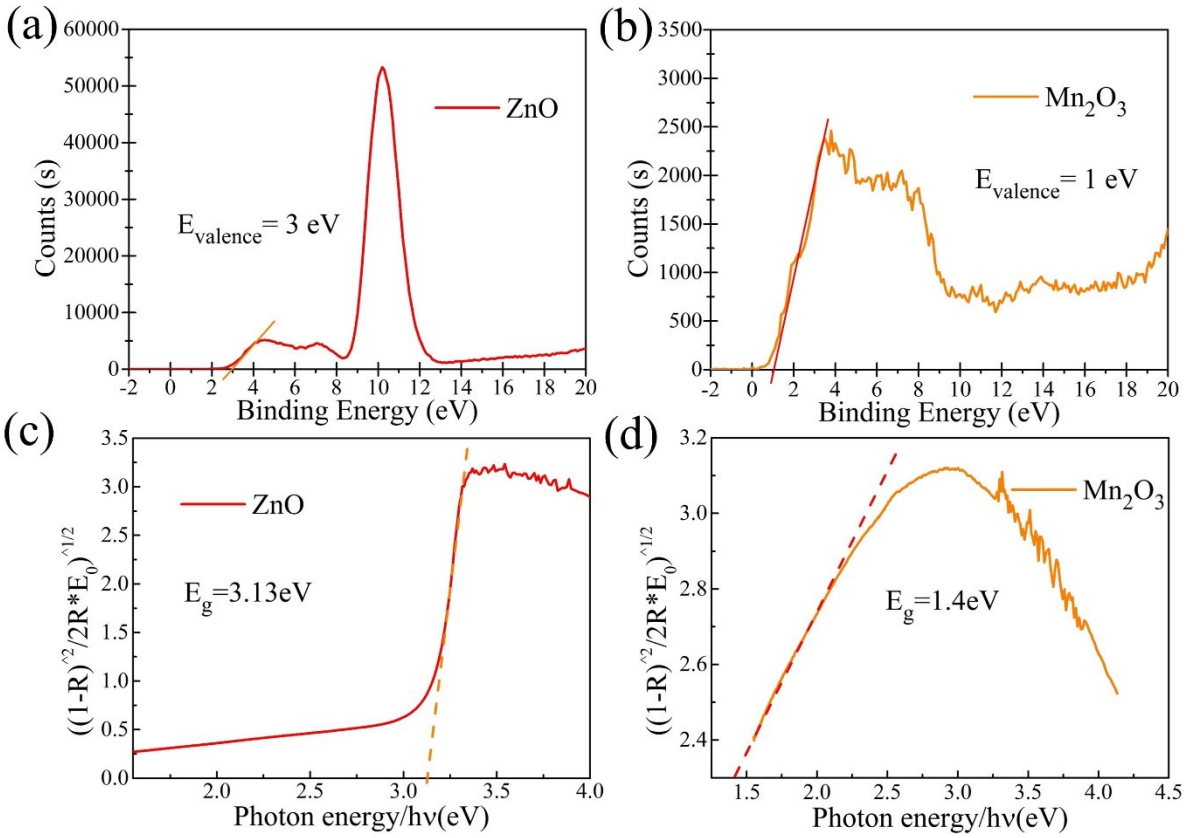

Fig. S4 The valence band spectra of (a) ZnO and (b) Mn_2O_3. The Band-gap energy of (c) ZnO and (d) Mn_2O_3.

As can be observed, the valence band edges of ZnO (Fig. S4 (a)) and Mn2O3 (Fig. S4 (a)) are located at +3 eV and +1 eV, while the band-gap width of them ((Fig. S4 (c) and (d)) are 3.13 eV and 1.4 eV, respectively. Thus the conduction band edges are located at about -0.13eV and -0.4 eV respectively.

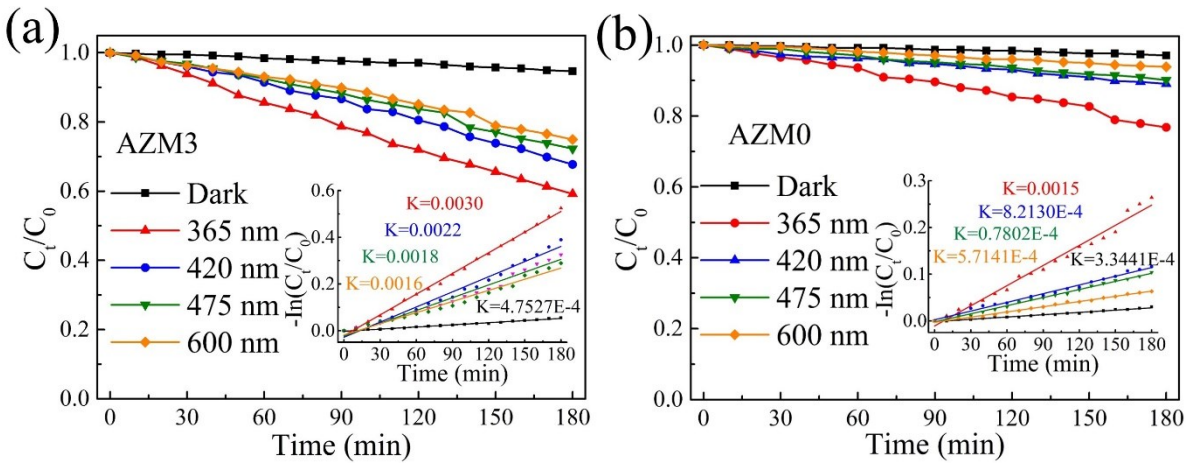

Fig. S5 Photodegradation curves and the corresponding first-order constants (K= ln(C0/Ct)) of as-synthesized (a) AZM3 samples, (b) AZM0 for the elimination of MB using single wavelength light source (including 365 nm, 420 nm, 475 nm and 600 nm).

As can be observed in Fig. S5, compared to the use of simulated sunlight, both of the photodegradation performances of AZM0 and AZM3 are visibly slow down to remove MB dye under monochromatic light irradiation, which result from the most of the energy was filtered out. The catalyst efficiency of AZM3 (as shown in Fig. S5a) is much higher than that of AZM0 (Fig. S5b) whether under ultraviolet or visible monochromatic light illumination, even in the dark environment. Particularly, under 420 nm light irradiation, the degradation efficiency for MB of AZM3 sample is about 2 times than that of AZM0, while it is one order of magnitude higher than AZM0 upon exposure to the monochromatic visible light. Above results indicate that the synergetic effects of Ag and Mn_2O_3 on ZnO enable to further optimize the photocatalytic capacity of Ag/ZnO, especially the light response in the visible region, which correspond well with the UV-vis and SPV results. In addition, For AZM0 and AZM3 samples, the photocatalytic activity decreased with the decreasing wavelength of the incident light source, this can be interpreted as the shorter the wavelength, the higher the energy, thus the more efficient separation of photogenerated carriers.